

Lecture Notes in Mechanical Engineering

Krishna Mohan Singh

Sushanta Dutta

Sudhakar Subudhi

Nikhil Kumar Singh *Editors*

Fluid Mechanics and Fluid Power, Volume 4

Select Proceedings of FMFP 2022

 Springer

Lecture Notes in Mechanical Engineering

Series Editors


Fakher Chaari, National School of Engineers, University of Sfax, Sfax, Tunisia

Francesco Gherardini , Dipartimento di Ingegneria “Enzo Ferrari”, Università di Modena e Reggio Emilia, Modena, Italy

Vitalii Ivanov, Department of Manufacturing Engineering, Machines and Tools, Sumy State University, Sumy, Ukraine

Mohamed Haddar, National School of Engineers of Sfax (ENIS), Sfax, Tunisia

Editorial Board

Francisco Cavas-Martínez , Departamento de Estructuras, Construcción y Expresión Gráfica Universidad Politécnica de Cartagena, Cartagena, Murcia, Spain

Francesca di Mare, Institute of Energy Technology, Ruhr-Universität Bochum, Bochum, Nordrhein-Westfalen, Germany

Young W. Kwon, Department of Manufacturing Engineering and Aerospace Engineering, Graduate School of Engineering and Applied Science, Monterey, CA, USA

Justyna Trojanowska, Poznan University of Technology, Poznan, Poland

Jinyang Xu, School of Mechanical Engineering, Shanghai Jiao Tong University, Shanghai, China

Lecture Notes in Mechanical Engineering (LNME) publishes the latest developments in Mechanical Engineering—quickly, informally and with high quality. Original research or contributions reported in proceedings and post-proceedings represents the core of LNME. Volumes published in LNME embrace all aspects, subfields and new challenges of mechanical engineering.

To submit a proposal or request further information, please contact the Springer Editor of your location:

Europe, USA, Africa: Leontina Di Cecco at Leontina.dicecco@springer.com

China: Ella Zhang at ella.zhang@springer.com

India: Priya Vyas at priya.vyas@springer.com

Rest of Asia, Australia, New Zealand: Swati Meherishi at swati.meherishi@springer.com

Topics in the series include:

- Engineering Design
- Machinery and Machine Elements
- Mechanical Structures and Stress Analysis
- Automotive Engineering
- Engine Technology
- Aerospace Technology and Astronautics
- Nanotechnology and Microengineering
- Control, Robotics, Mechatronics
- MEMS
- Theoretical and Applied Mechanics
- Dynamical Systems, Control
- Fluid Mechanics
- Engineering Thermodynamics, Heat and Mass Transfer
- Manufacturing Engineering and Smart Manufacturing
- Precision Engineering, Instrumentation, Measurement
- Materials Engineering
- Tribology and Surface Technology

Indexed by SCOPUS, EI Compendex, and INSPEC.

All books published in the series are evaluated by Web of Science for the Conference Proceedings Citation Index (CPCI).

To submit a proposal for a monograph, please check our Springer Tracts in Mechanical Engineering at <https://link.springer.com/bookseries/11693>.

Krishna Mohan Singh · Sushanta Dutta ·
Sudhakar Subudhi · Nikhil Kumar Singh
Editors

Fluid Mechanics and Fluid Power, Volume 4

Select Proceedings of FMFP 2022

 Springer

Editors

Krishna Mohan Singh
Department of Mechanical and Industrial
Engineering
Indian Institute of Technology Roorkee
Roorkee, Uttarakhand, India

Sushanta Dutta
Department of Mechanical and Industrial
Engineering
Indian Institute of Technology Roorkee
Roorkee, Uttarakhand, India

Sudhakar Subudhi
Department of Mechanical and Industrial
Engineering
Indian Institute of Technology Roorkee
Roorkee, Uttarakhand, India

Nikhil Kumar Singh
Department of Mechanical and Industrial
Engineering
Indian Institute of Technology Roorkee
Roorkee, Uttarakhand, India

ISSN 2195-4356

ISSN 2195-4364 (electronic)

Lecture Notes in Mechanical Engineering

ISBN 978-981-99-7176-3

ISBN 978-981-99-7177-0 (eBook)

<https://doi.org/10.1007/978-981-99-7177-0>

© The Editor(s) (if applicable) and The Author(s), under exclusive license to Springer Nature Singapore Pte Ltd. 2024

This work is subject to copyright. All rights are solely and exclusively licensed by the Publisher, whether the whole or part of the material is concerned, specifically the rights of translation, reprinting, reuse of illustrations, recitation, broadcasting, reproduction on microfilms or in any other physical way, and transmission or information storage and retrieval, electronic adaptation, computer software, or by similar or dissimilar methodology now known or hereafter developed.

The use of general descriptive names, registered names, trademarks, service marks, etc. in this publication does not imply, even in the absence of a specific statement, that such names are exempt from the relevant protective laws and regulations and therefore free for general use.

The publisher, the authors, and the editors are safe to assume that the advice and information in this book are believed to be true and accurate at the date of publication. Neither the publisher nor the authors or the editors give a warranty, expressed or implied, with respect to the material contained herein or for any errors or omissions that may have been made. The publisher remains neutral with regard to jurisdictional claims in published maps and institutional affiliations.

This Springer imprint is published by the registered company Springer Nature Singapore Pte Ltd.

The registered company address is: 152 Beach Road, #21-01/04 Gateway East, Singapore 189721, Singapore

Paper in this product is recyclable.

Contents

Combustion

Numerical Analysis on the Effect of Aspect Ratio in a Diesel Injector Using Diesel and Diesel–Ethanol Blend	3
Aiswarya A. Satheesan, Nikhil Prasad, Nevin Nelson, S. Niranjana, and Anjan R. Nair	
Numerical Simulation of Gasification and Plasma Pyrolysis Process for Lignite Coal: A Comparative Study	17
Sidhartha Sondh, Darshit S. Upadhyay, Sanjay Patel, and Rajesh N. Patel	
Availability Analysis of Diesel-Powered CI Engines with Single and Multiple Injection Strategies	27
Ketan V. Warghat, Aditya Tiwari, B. Yogesh, G. M. Nayak, B. Saravanan, and Pankaj S. Kolhe	
Change in Vortex Breakdown Mode and Its Influence on Flame Shape of a Co/counter Concentric Swirling Streams	41
Atanu Dolai, Prasad Boggavarapu, and R. V. Ravikrishna	
Entrained Dust Combustion in Pre-Heated Air	53
Mohd. Tousif, A. Harish, and V. Raghavan	
An Experimental Investigation into the GDI Spray Characteristics of Ethanol and Lemon Peel Oil	67
G. M. Nayak, B. Abinash, B. Yogesh, V. W. Ketan, P. S. Kolhe, and B. Saravanan	
Numerical and Experimental Performance Comparison of a Typical Swirl Co-Axial Injector for a Cryogenic Combustor	81
R. Sujithkumar, K. Chenthil Kumar, K. R. Anil Kumar, T. Jayachandran, and Kowsik Bodi	

Analytical Modelling of Effect of Steam Dilution on Hydrogen Combustion and Application to a Typical Nuclear Reactor Containment	95
Aditya Karanam, Vishnu Verma, and J. Chattopadhyay	
Thermal Performance of a Single-Layer Porous Radiant Burner with Biogas as Fuel: A Numerical Study	109
Ayush Painuly and Niraj K. Mishra	
Numerical Validation and Benchmarking of Hydrogen Flame Propagation in a Vertical Acceleration Tube Experimental Facility	119
Aditya Karanam, Vishnu Verma, and J. Chattopadhyay	
Detailed Chemical Kinetics Mechanism for Condensed Phase Decomposition of Ammonium Perchlorate	133
Jay Patel, Prathamesh Phadke, Rohit Sehrawat, Arvind Kumar, Arindrajit Chowdhury, and Neeraj Kumbhakarna	
Onset of Thermoacoustic Oscillations in an Annular Combustor with Flames Stabilized by Circular Discs	145
Balasundaram Mohan and Sathesh Mariappan	
Development of Advanced Fuel Injector Concepts for Compact Lean-Burn Gas-Turbine Combustors	157
Ayush Divyansh, Preetam Jamod, and K. P. Shanmugasadas	
Experimental Study on GDI In-Cylinder Combustion Quality of Ethanol and Lemon Peel Oil	171
B. Abinash, B. Yogesh, G. M. Nayak, V. W. Ketan, P. S. Kolhe, and B. Saravanan	
Numerical Study on Soot Formation of Methyl Methacrylate Pool Flames with Coflow Air	185
Argha Bose, D. Shanmugasundaram, and V. Raghavan	
Impact of Computational Domain and Cell Type on Large Eddy Simulations in OpenFOAM for a Turbulent Partially Premixed Flame	197
Sandeep Lamba and Krishna Kant Agrawal	
Exergy Analysis of Deflagration Wave Propagating in Autoignitive H₂ Mixture for Constant Pressure Boundary Conditions	213
Rahul Patil and Sheshadri Sreedhara	
Numerical Investigation of Combustion Dynamics in a Multi-element Combustor Using Flamelet Approach	225
Abhishek Sharma, Ashoke De, Varghese M. Thannickal, T. John Tharakan, and S. Sunil Kumar	

Experimental Investigations on Emissions and Performance of Spark Ignition Engine Fuelled with Butanol–Pentane–Gasoline Blends 241
 Parag P. Mangave, Vishal V. Patil, Nilesh D. Pawar, and Ranjit S. Patil

CFD Analysis of Afterburner with Convergent–Divergent Nozzle for Various Air–Fuel Ratios 253
 Gurrala Srinivasa Rao

Computational Analysis of the Thermo Hydrodynamic Characteristics in a Can-Type Gas Turbine Combustor 269
 Mohit Bansal, Satyam Dewivedi, and Abdur Rahim

Experimental Study of Acoustic Phenomenon in a Closed Combustion Chamber 279
 A. Ananthkrishnan, Siba Prasad Choudhury, S. Syam, and Ratan Joarder

The Effect of Lean Premixed Combustion on Thermoacoustic Instability in a Swirl Combustor 289
 Subhash Kumar, Sanjeev Kumar, and Sheshadri Sreedhara

Computational Modelling of MMH/NTO Combustion in a Multi-element Triplet Injector Combustor 301
 Abhishek Sharma, Varghese M. Thannickal, T. John Tharakan, and S. Sunil Kumar

Microfluidics

Novel Tree Branching Microchannel Heat Sink Under Variable and Constant Fluid Volume Approaches 319
 Sangram Kumar Samal and Sandip Kumar Saha

Two-Dimensional, Magnetic Actuation of Ferrofluid Droplet on an Open-Surface Microfluidic Platform 333
 Debiprasad Chakrabarty, Niladri Chakraborty, and Ranjan Ganguly

Numerical Analysis of Heat Transfer and Fluid Flow in Microchannel Heat Sinks Designed for Uniform Cooling 345
 Shivayya C. Hiremath, Rohit Kumar, Arman Mohaddin Nadaf, and Manmohan Pandey

Numerical Investigation on Hydrodynamics of Lubricant-Infused Hydrophobic Microchannel with Transversely Oriented Cavities 357
 Adarsh R. Nair, K. Nandakumar Chandran, and S. Kumar Ranjith

Effect of Microstructures in the Flow Passage on the Flow Dynamics of Microchannel 369
 A. Rajalingam and Shubhankar Chakraborty

Combined Effect of Heterogeneous Zeta Potential on Microchannel Wall and Conductive Link in Induced Charge Electrokinetic Micromixing	381
Anshul Kumar Bansal, Ram Dayal, and Manish Kumar	
Analysis of Sperm Cell Kinetics in Newtonian and Non-Newtonian Fluid Medium Within a Microfluidic Channel	395
Dhiraj B. Puri, Vadiraj Hemadri, Arnab Banerjee, and Siddhartha Tripathi	
Conjugate Heat Transfer Analysis of U-Bend/Turn Microchannel: A Computational Approach	409
Jyoti Ranjan Mohapatra and Manoj Kumar Moharana	
Experimental Investigation of Fluid Flow Behaviour in Parallel Microchannel Using Micro-PIV	425
Rohit Kumar, Chandan Nashine, Arman Mohaddin Nadaf, Mohd Sakib Hussain, and Manmohan Pandey	
Study of Path Selection of a Droplet in a Symmetric Y-Microchannel Using a Uniform Electric Field	437
Satya P. Pandey, Sandip Sarkar, and Debashis Pal	
Microfluidic Solute Transport by Interference of Oscillatory Thermal Marangoni Effect and Patterned Wall Slip	449
Shubham Agrawal, Prasanta K. Das, and Purbarun Dhar	
Analysis of Micro-nozzle Flow Using Navier–Stokes and DSMC Method and Locating the Separation Plane Based on Modified Knudsen Number	461
Ashok Kumar, Manu K. Sukesan, and Shine S. R.	
Parametric Study on the Primitive Lattice Using the Pore-Scale Simulation to Characterize the Flow and Heat Transfer Performance	475
Surendra Singh Rathore, Balkrishna Mehta, Pradeep Kumar, and Mohammad Asfer	
Experimental and Numerical Studies on Liquid Bridge Stretching in Uni-port Lifted Hele-Shaw Cell for Spontaneous Fabrication of Well-Like Structures	491
Makrand Rakshe, Sachin Kanhurkar, Amitabh Bhattacharya, and Prasanna Gandhi	
Numerical Investigation on Inertial Migration of Spherical Rigid Particle in the Entrance Region of a Microchannel	501
K. K. Krishnaram and S. Kumar Ranjith	

Dynamics of Electrically Actuated Carreau Fluid Flow in a Surface-Modulated Microchannel 513
 Subhajyoti Sahoo and Ameeya Kumar Nayak

Heat Transfer Analysis of Peltier-Based Thermocycler for a Microfluidic-PCR Chip 527
 Nikhil Prasad, B. Indulakshmi, R. Rahul, and Ranjith S. Kumar

Effect of Viscosity on the Margination of White Blood Cells in an Inertial Flow Microfluidic Channel 543
 Dhiren Mohapatra, Rahul Purwar, and Amit Agrawal

Experimental Investigation of Two-Phase Immiscible Liquid Flow Through a Microchannel 553
 Rohit Kumar, Chandan Nashine, Arman Mohaddin Nadaf, Harish Kumar Tomar, and Manmohan Pandey

Elastohydrodynamics of Electromagnetically Actuated Deformable Microfluidic Systems 563
 Apurba Roy and Purbarun Dhar

Experimental and Numerical Analysis of Ferrofluid in Partially Heated Closed Rectangular Microchannel Tube Under Non-uniform Magnetic Field 577
 Ramesh Kumar, Shivam Raj, and S. K. Dhiman

Numerical Investigation on the Effect of Reynolds Number on the Droplet Bypass Through T-Junction Using Lattice Boltzmann Method 591
 T. Sudhakar, Arup K. Das, and Deepak Kumar

Bio-fluid Mechanics

Blood Flow Modeling in Stenosed Arteries Using CFD Solver 605
 Priyambada Praharaj, Chandrakant Sonawane, and Vikas Kumar

Highlighting the Importance of Nasal Air Conditioning in Septoplasty Using Virtual Correction Tools: A Numerical Study 619
 Kartika Chandra Tripathy and Ajay Bhandari

Thrombosis Modelling in a Stenosed Artery 633
 Prateek Gupta, Rakesh Kumar, Sibasish Panda, and Mohammad Riyan

Gold Nanoparticle-Antibody Bio-Probe Analysis: Synthesis, Conjugation, Characterization and Dot Blot Assay on Paper 643
 Prateechee Padma Behera, Shubham Kumar, Monika Kumari, Pranab Kumar Mondal, and Ravi Kumar Arun

A Computational Analysis of the Impact of Blood’s Viscoelastic Properties on the Hemodynamics of a Stenosed Artery 655
 Sourabh Dhawan, Pawan Kumar Pandey, Malay Kumar Das, and Pradipta Kumar Panigrahi

Effect of Induced Helicity on the Hemodynamics of Carotid Artery Passage 671
 L. Rakesh, Arun Kadali, K. Prakashini, and S. Anish

Numerical Simulation of Flow in an Idealized Intracranial Aneurysm Model to Study the Effect of Non-newtonian Blood Flow Rheology 685
 Suraj Raj, S. Anil Lal, and Anjan R. Nair

On the Replication of Human Skin Texture and Hydration on a PDMS-Based Artificial Human Skin Model 699
 Aditya Ranjan, Vijay S. Duryodhan, and Nagesh D. Patil

Simulation of Lateral Migration of Red Blood Cell in Poiseuille Flow Using Smoothed Particle Hydrodynamics 709
 Justin Antony and Ranjith Maniyeri

Effect of Stenosis Severity on the Hemodynamics of an Idealized Straight Arterial Tube 723
 Pawan Kumar, Somnath Roy, and Prasanta Kumar Das

Microdevice for Plasma Separation and in Vitro Quantification of Plasma Proteins 735
 Tony Thomas, Neha Mishra, and Amit Agrawal

White Blood Cell Separation and Blood Typing Using a Spiral Microdevice 745
 Sanjay Mane, Vadiraj Hemadri, Sunil Bhand, and Siddhartha Tripathi

Effect of Arterial Flow on Heat Transfer During Magnetic Hyperthermia Application 755
 Subeg Singh and Neeraj Kumar

Flow Separation and Pressure Drop Analysis for Blood Flow in Symmetric Stenosed Arteries of Various Shapes 767
 Anamika Maurya, Janani Sree Murallidharan, and Atul Sharma

Comparative Study of Uniform and Pulsatile Blood Flow Through Single Stenosed Carotid Artery 781
 Swapnil Rajmane and Shaligram Tiwari

Image-Based Retinal Haemodynamics Simulation of Healthy and Pathological Retinal Vasculature 797
 Shivam Gupta and Ajay Bhandari

Numerical Study on the Effect of Exercise on Various Configurations of Stenosis in Coronary Artery 809
 Siddharth D. Sharma, Piru Mohan Khan, Suman Chakraborty, and Somnath Roy

Effect of Aging on Passive Drug Diffusion Through Human Skin 823
 Aditya Ranjan, Vijay S. Duryodhan, and Nagesh D. Patil

Computational Investigation on the Empirical Relation of Murray’s Law 837
 Mudrika Singhal and Raghvendra Gupta

Investigation of Impulse Jet Dispersion Mechanism of Needle-Free Drug Delivery Device 847
 Priyanka Hankare, Sanjeev Manjhi, and Viren Menezes

Analysis of 2D Human Airway in Laminar and Turbulent Flow Model 855
 Vivek Kumar Srivastava and Aman Raj Anand

Effects of Stenosis Profile on Hemodynamic and Mass Transport in Axisymmetric Geometries: A Numerical Study 865
 Ankani Sunil Varma and K. Arul Prakash

Experimental and Numerical Study of Flow Through Ventilator Splitter 875
 Aniruddh Mukunth, Raj Shree Rajagopalan, and Naren Rajan Parlikkad

Bioconvective MHD Flow of Micropolar Nanofluid Over a Stretching Sheet Due to Gyrotactic Microorganisms with Internal Heat Generation/Absorption and Chemical Reaction 891
 P. Vimala and R. Dhivyalakshmi

Machine Learning in Fluid Mechanics

Application of Machine Learning for Forced Plume in Linearly Stratified Medium 909
 Manthan Mahajan, Nitin Kumar, Deep Shikha, Vamsi K. Chalamalla, and Sawan S. Sinha

Comparative Study of Future State Predictions of Unsteady Multiphase Flows Using DMD and Deep Learning 923
 Neil Ashwin Raj, Danesh Tafti, Nikhil Muralidhar, and Anuj Karpatne

Deep Learning Approach to Predict Remaining Useful Life of Axial Piston Pump 937
 Md Adil and Pratik Punj

Machine Learning-Assisted Modeling of Pressure Hessian Tensor 949
 Deep Shikha and Sawan S. Sinha

About the Editors

Prof. Krishna Mohan Singh is Professor in the Department of Mechanical and Industrial Engineering at Indian Institute of Technology (IIT) Roorkee. His research interests include the areas of computational mechanics, development of novel parallel algorithms, meshfree methods, shape and topology optimization, fluid dynamics, DNS/LES of turbulent flows, CAE, computer-aided analysis and design of thermo-fluid and multi-physics systems, computational fluid dynamics, modeling and simulation of flow and heat transfer in turbomachines, transport and energy systems.

Prof. Sushanta Dutta is Professor in the Department of Mechanical and Industrial Engineering at Indian Institute of Technology (IIT) Roorkee. His research interests are in the areas of experimental fluid mechanics, experimental heat transfer, optical measurement techniques, active and passive control of flow field, wake dynamics, turbulence study, Schlieren, HWA, PIV, LCT, PSP, microfluidics and heat transfer augmentation using phase change material.

Prof. Sudhakar Subudhi is Professor in the Department of Mechanical and Industrial Engineering at Indian Institute of Technology (IIT) Roorkee. His research interests are in the area of experimental heat transfer and fluid mechanics, heat transfer enhancement of natural and forced convection in water/nanofluids, natural ventilation and unconventional energy systems.

Dr. Nikhil Kumar Singh is Assistant Professor in the Department of Mechanical and Industrial Engineering at Indian Institute of Technology (IIT) Roorkee. His broad research interests include direct numerical simulations of two-phase flows and phase change, computational fluid dynamics and heat transfer, numerical methods and turbulent flows.

Combustion

Numerical Analysis on the Effect of Aspect Ratio in a Diesel Injector Using Diesel and Diesel–Ethanol Blend



Aiswarya A. Satheesan, Nikhil Prasad, Nevin Nelson, S. Niranjana, and Anjan R. Nair

Abstract In direct injection diesel engines, spray optimization greatly enhances efficiency and low emissions combustion. The flow inside an injector impacts the process of spray, combustion, and exhaust. The nozzle shape and spray determine the atomization and the outlet engine emissions. The results were obtained for spray characteristics of diesel and ethanol–diesel blend in a nozzle injector with aspect ratios varying from 1, 1.2, 1.4, and 1.6. Parameters, such as spray penetration length, spray angle, and spray characteristics including the Sauter mean diameter (SMD), the De Brouckere diameter, the mean diameter and volume, and particle velocity, were investigated and revealed a strong dependence on modifications in the aspect ratio of the nozzle orifice. Simulation of atomization model was carried out and compared using discrete phase model (DPM) using computational fluid dynamics (CFD) modeling. Additionally, validation from the experiment finding results is also provided. Elliptical C was observed to have a minimum SMD up to 28.04% and a minimum De Brouckere diameter up to 28.63%. Ethanol–diesel blend showed best spray parameters when considering the macroscopic spray properties and the drop size distribution. Moreover, under non-evaporative conditions, the tested fuel ethanol–diesel Blend exhibited better spray characteristics and better cavitation phenomenon of 12.13% at higher aspect ratios than at lower ones. In addition, elliptical nozzle spray had a higher spray cone angle than circular nozzle spray.

Keywords Aspect ratio · Spray simulation · Elliptical nozzle

A. A. Satheesan · N. Prasad · N. Nelson · S. Niranjana · A. R. Nair (✉)
Department of Mechanical Engineering, College of Engineering, Trivandrum 695016, India
e-mail: anjan@cet.ac.in

N. Nelson
Department of Mechanical Engineering, Bishop Jerome Institute (Affiliated to A P J Abdul Kalam Technological University), Kollam, India

1 Introduction

Diesel engines are frequently utilized as the primary power source for the road transportation sector. Because of their outstanding thermal efficiency, operational dependability, and durability, the greater understanding of effective fuel use and automotive pollution reduction, which led to enhanced modern direct injection engines like strengthening the spray breakup and generating smaller droplets, has greatly assisted research on the fluid behavior of fuel injection nozzles [1].

Atomization and fuel spray properties in direct injection engines are critical, particularly for gas emissions and combustion efficiency; these factors significantly impact the spray's shape, atomization quality, engine performance, and emission characteristics. So, the jet breakup inside the chamber also influences the subsequent processes of ignition, combustion, and pollutant generation. Therefore, it's crucial to consider the fuel injector nozzle effect and the features of the spraying technique with different fuel types. The injector nozzle is a crucial component in a diesel engine. The elliptical orifice diesel nozzle has the potential to improve spray quality and air– fuel mixing [2].

Liquid sprays have been the subject of extensive research due to their actual relevance and the challenges in predicting their behavior from basic principle. While some sprays are composed of several short pulses and may never reach a steady state, others are continuous and stable, at least after a brief start-up transient.

Alcohols, like other oxygenated fuels, enhance complete combustion and reduce particulate matter (PM), carbon monoxides (CO), and unburned hydrocarbon emissions (HC) [3]. Reduced SMD and larger spray angle was achieved by implementing elliptical-shaped sprays. Further study can be done on the impact of alternative fuels on the spray, performance, and regarding diesel engines' emission characteristics, which affect engines parameters performance and emissions

2 Literature Review and Objective

Many researchers and pioneers worldwide have investigated diesel fuel injectors and their influence. The discrete phase model (DPM) was developed to investigate the cavitation process in fuel injectors and the macro spray characteristics of three different types of nozzle spray shapes using diesel and hybrid biofuel blends at various injection pressures and backpressures. The findings of the nozzle simulation study showed that the nozzle spray morphology had a greater influence on the cavitation area than the fuel type [4].

A numerical analysis on the fuel spray behavior and fluctuation of spray characteristics in internal combustion engines were investigated, and it was observed that the fuel spray is impacted by the cavitation phenomena in diesel engines. More bubbles are generated when cavitation is severe [5].

An experimental study on the biodiesel spray liquid-phase behaviors of elliptical and circular nozzles revealed that under steady-state conditions, the elliptical nozzle spray liquid-phase penetration is smaller than the circular one [6]. The elliptic orifice diesel nozzle can improve spray and air–fuel mixing quality, significantly impacting diesel engine combustion and emissions. In all view planes, the elliptical spray had a wider spread of particles than the circular spray, and the circular orifice's spray cone angle was consistently smaller than that of the elliptical orifice [7].

The spray liquid breakdown behavior of a diesel nozzle with non-circular cross-sectional geometries was investigated experimentally under evaporative conditions, and the impact of varied injection pressures and bulk temperatures. In both geometric cases, the study demonstrated that injection pressure has less impact on the penetration of liquid spray. Increasing the ambient temperature, on the other hand, can reduce spray- liquid penetration [8]. Since ethanol is an oxidized fuel, the oxygen level of the mix fuel rises, increasing the thermal efficiency of the engine's brakes. The thermal efficiency increased by 3.63% while the cylinder pressure increased by 0.46%, when the ethanol content reached 20% at full load [9].

An efficient approach for determining the true extent of vapor zones and turbulence intensity was devised using a comprehensive model for cavitating flow in conjunction with the CFD-ACE+ code was introduced. Cavitation flow involves phase transition. And was shown to be sensitive to the development and motion of vapor bubbles, turbulent oscillations in pressure, velocity, and the quantity of non- condensable gases dissolved or consumed in the operating liquid [10].

Numerical simulation of spray was modeled to study the effect of cavitation on the quality and characteristics of spray, such as penetration length and Sauter mean diameter of the nozzle's specific geometry. Smaller droplets produced by this spray will improve and help accelerate combustion, enhance power and torque, and reduce outlet emissions [11].

The CFD-programmed software CONVERGE incorporates a recently developed primary breakdown model (KH-ACT) for detailed engine simulations. KH-ACT takes into account the effects of the turbulence and cavitation created inside the injector nozzle. The conical and hydroground nozzle inner nozzle flow impacts of orifice geometry were analyzed. The analysis indicated that the reduced vaporization rate and air–fuel mixing could cause an earlier ignition of the nozzle downstream [12].

The aspect ratio of the elliptical nozzle improved the aerodynamic and penetration characteristics differently, but the optimum/maximum allowable aspect ratio for better aerodynamic characteristics was not reported. Only two types of fuel (diesel/ biofuel) were used to characterize the fuel injector nozzle effect. The mechanism of the liquid fuel breaking up, atomization, and size of the droplet is unclear near the nozzle's exit.

The objective of the study is to investigate the effect of fuel spray characteristics and variation for two types of fuels: Diesel and the combination of diesel and ethyl alcohol (ethanol), using numerical simulation approaches and to numerically evaluate the relationship between the Sauter mean diameter (SMD), De Brouckere diameter

D [3, 4], mean diameter, and volume spray parameters relation to the aspect ratio of the nozzle and the cavitation phenomenon.

3 Physical Model and Domain

The project aims to understand the spray characteristics inside a diesel injector nozzle with preliminary assumptions of unsteady 3D incompressible turbulent nozzle flow and obeying no-slip conditions (fluid velocity at the walls equals the wall velocity) were run with a commercial fluid dynamic code.

The discrete phase model (DPM) was introduced to study the fuel injector process and the macro spray characteristic of the injector. The Ansys Design modeler does the 3D model of the elliptical diesel injector. The commercial CFD software Ansys Fluent 2020 R1 performs the numerical simulation. The Standard $k - \varepsilon$ is chosen as the viscous model.

3.1 Governing Equations

The problem considered is the spray simulation of a diesel injector by varying the aspect ratios of the orifice and also different fuels are used. The analysis is going to be carried out on an incompressible fluid with unsteady-state condition. The governing equations for the 3D continuous flow of the fuel in the injector consist of the continuity, momentum, and energy equation that solved the Navier–Stokes equations. The equations are listed as follows:

Continuity equation

$$\frac{D\rho}{Dt} + \rho \nabla \cdot \vec{v} = 0 \quad (1)$$

Conservation of momentum

$$\rho \frac{D}{Dt} v = -\nabla p + \mu \nabla^2 v + \rho g \quad (2)$$

3.2 Geometry Details

The injector is coupled with an injection chamber (exit diameter = 5.1925 mm) with a nozzle hole to length diameter ratio of 0.280. The 3D design was drawn using ANSYS Workbench 20.0 using design modeler.

Diesel fluid with a density of 730 kg/m^3 and a viscosity of 0.0024 kg/ms is chosen as the fuel. For diesel–ethanol blend, the viscosity is 0.0018 kg/ms , and the density is 807 kg/m^3 . The droplet surface tension is 0.026 and 0.0306 N/m for diesel and diesel–ethanol blends, respectively. A singular spray jet is modeled, and the injection takes from the center of the inlet.

3.3 Grid Independence Study

The optimum number of grids must be specified in order to execute additional research and calculations. The calculated results ought to be grid-independent and never fluctuate as the number of cells changes (Table 1).

For four distinct body sizes, grid independence research was conducted. From 0.2 and 0.02 body sizing onwards, the penetration length is steady. In the case of SMD, there was no significant modification when the number of nodes and elements were increased beyond 336,176 and 323,752, respectively. As a result, body sizes of 0.1 and 0.01 were found to be appropriate (Figs. 1 and 2).

Table 1 Variation of penetration length and SMD with number of cells

Body sizing → 1 (mm)	Body sizing → 2 (mm)	No. of nodes	No. of elements	Penetration length (m)	Overall SMD (m)
0.4	0.025	11,506	10,200	0.008035	$2.253e - 7$
0.2	0.02	61,321	57,780	0.00814	$2.7743e - 7$
0.1	0.01	336,176	323,752	0.00814	$2.971e - 7$
0.05	0.005	2,065,186	2,021,865	0.00814	$3.00e - 7$

Fig. 1 Variation of SMD with no. of elements

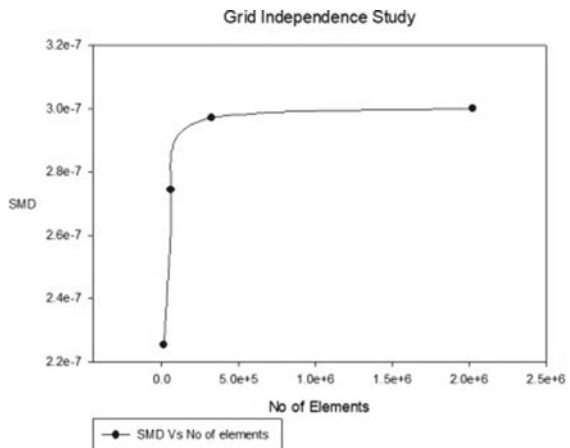
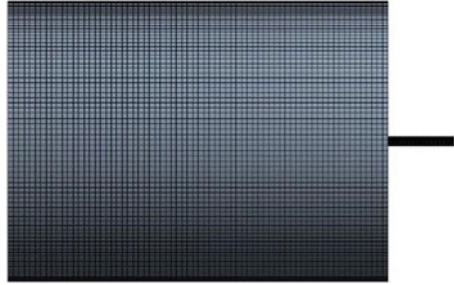


Fig. 2 Mesh generation

From the above figures, it is clear that SMD does not vary when number of elements is increased from 323,752. Therefore, further calculations and analysis, body sizing of 0.1 and 0.01 is taken for the geometry.

3.4 Mesh Generation

Mesh is generated using inbuilt meshing program inside ANSYS 20.0 in three dimensions. Cells are used to create a structured mesh that becomes finer as it moves from the cylinder's edge to its core. The mesh quality was found to be 0.95 which implies the model is having a good mesh quality.

The number of nodes and elements in the geometry after meshing are 336,176 and 323,752, respectively, chosen after obtaining results from the grid independence study plotted for penetration length versus the number of elements.

3.5 Boundary Condition

In the present geometry, the left side is defined as the inlet and the right side is defined as the outlet. The remaining surface is defined as the wall (Tables 2 and 3).

Table 2 Boundary conditions

Inlet pressure	100 MPa
Outlet pressure	1 MPa
Wall	No slip condition
Working fluid	i Diesel ii Combination of diesel and ethanol

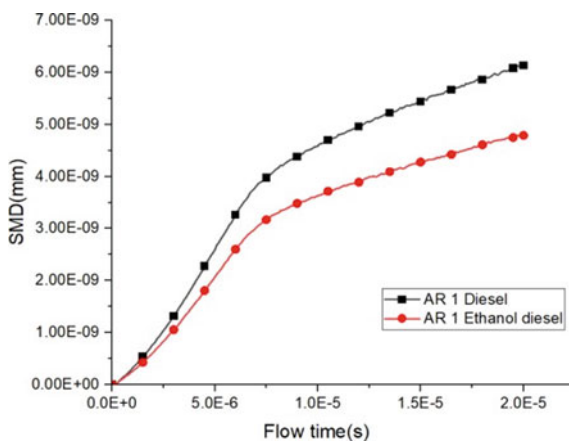
Table 3 Settings for spray simulation

Parameter	Quality
Injection pressure	100 MPa
Outlet pressure	1 MPa
Mass flow rate	3e – 6 kg/s
Injection duration	1 s
Injection type	Surface

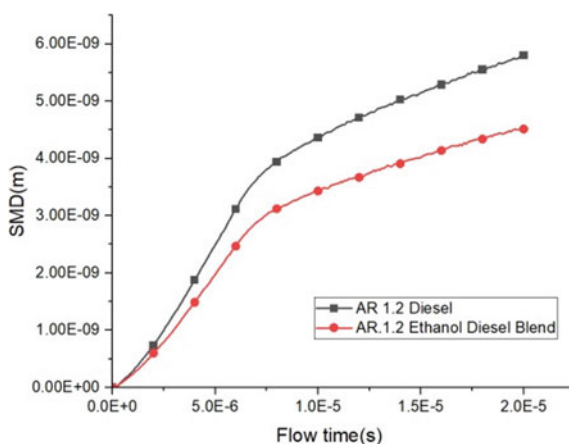
4 Results and Discussion

See Graphs 1, 2, 3 and 4.

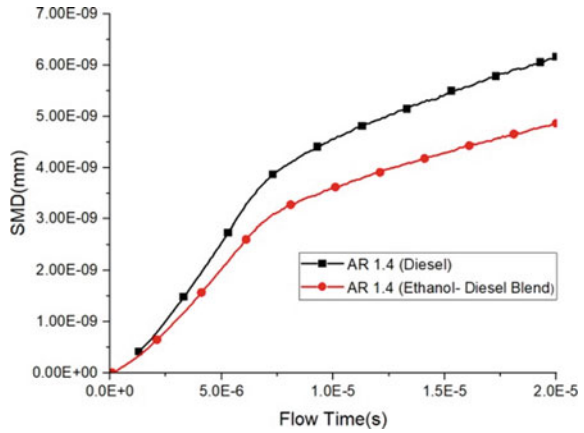
Graph 1 Comparison of SMD for aspect ratio 1



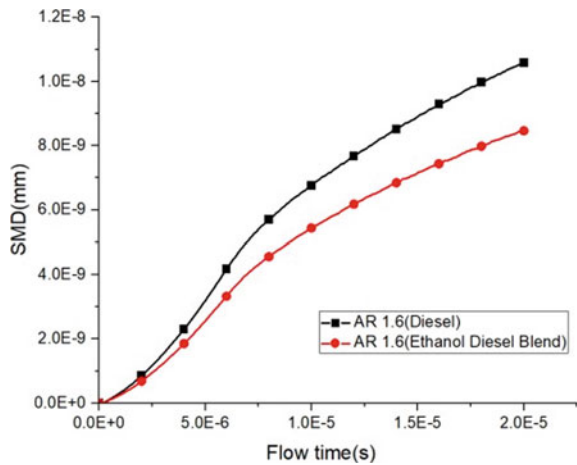
Graph 2 Comparison of SMD for aspect ratio 1.2



Graph 3 Comparison of SMD for aspect ratio 1.4



Graph 4 Comparison of SMD for aspect ratio 1.6



4.1 Effect on Sauter Mean Diameter (SMD)

The smaller the SMD, the evaporation and atomization process accelerates also it resulting in uniform size distribution and increased number of droplets. Therefore, it is of benefit to mixture formation. Due to diesel’s higher density, stronger intermolecular forces produce poor atomization. The difference in fuel viscosity and density is mostly responsible for the SMD variations between the fuels. Diesel exhibits larger droplet sizes than ethanol–diesel mixtures. Ethanol–diesel blends always have lower SMD and De Brouckere values than pure diesel. They get smaller as the quantity of diesel increases, while it randomly varies for variation in aspect ratio (Table 4).

Table 4 Spray angle obtained for various aspect ratios

Aspect ratio	Spray angle
1	12.32°
1.2	14.05°
1.4	15.33°
1.6	16.30°

Fig. 3 Spray angle for aspect ratio 1

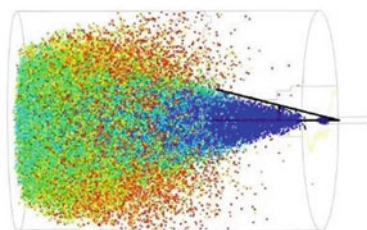
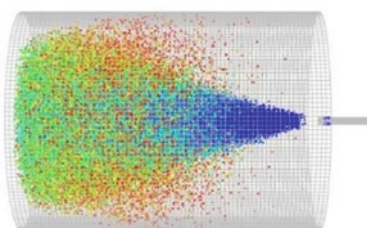


Fig. 4 Spray angle for aspect ratio 1.2



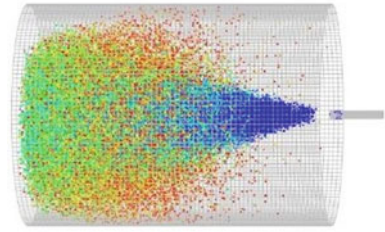
4.2 Effect on Spray Angle

An important parameter of fuel sprays is the angle of the spray's edge as it leaves the injector hole. For single sprays, the two lines tangent to the spray's margins, extending from the injection point, constitute the spray angle. Lower aspect ratios result in smaller spray angles, while higher aspect ratios, in comparison, result in wider spray angles. The particle residence time is tracked to determine the spray angle for the cases of a Circle, Elliptical A, B, And C, respectively is shown in Figs. 2, 3, 4 and 5. The circle's spray angle was found to be 12.32°, whereas the maximum spray angle was found to be 16.30° for Elliptical C.

4.3 Effect of Cavitation

Figures 6, 7, 8 and 9 show the variation of pressure contour for circular injector nozzle and Elliptical A, B, and C cases, respectively. The pressure contour shows

Fig. 5 Spray angle for aspect ratio 1.4



that in all cases of aspect ratio, cavitation bubbles first have been generated, close to the nozzle inlet's sharp corners. Then, the flow of spray transfers these bubbles downward in both an axial and radial direction. The main cause of this phenomena is the development of low-pressure zones. Because of the abrupt change in flow direction near sharp corners, even negative values were detected (Fig. 10).

Fig. 6 Spray angle for aspect ratio 1.6

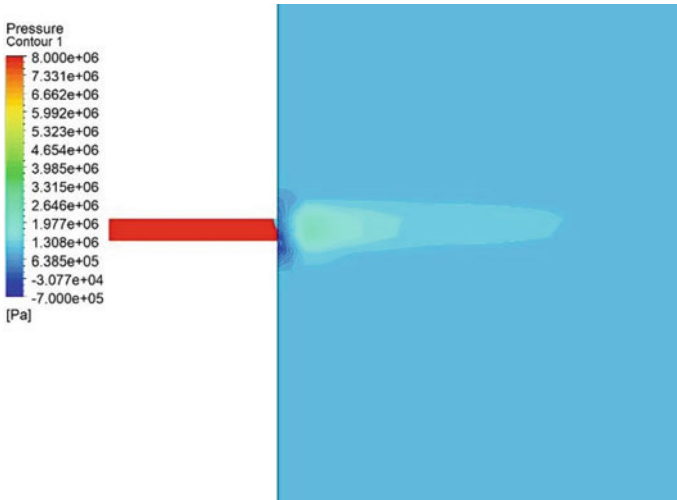
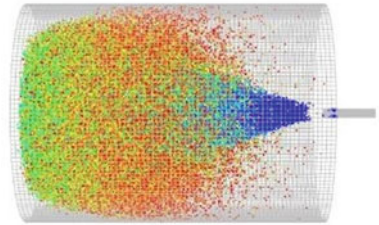


Fig. 7 Pressure contour for aspect ratio 1

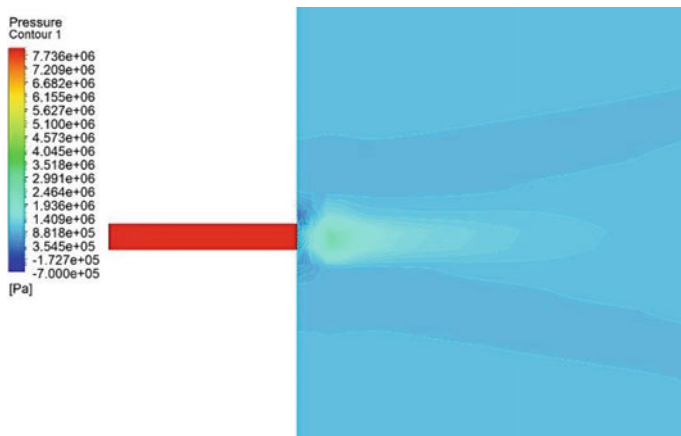


Fig. 8 Pressure contour for aspect ratio 1.2

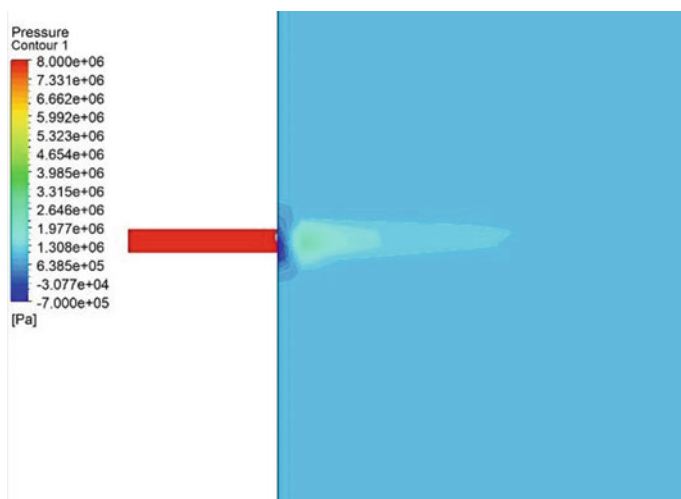


Fig. 9 Pressure contour for aspect ratio 1.4

The formation of cavitation inside the nozzle can be enhanced by an increase in aspect ratio. The cavitation intensity was more intensive for Elliptical B and C as compared to other nozzle shapes for the same injection time

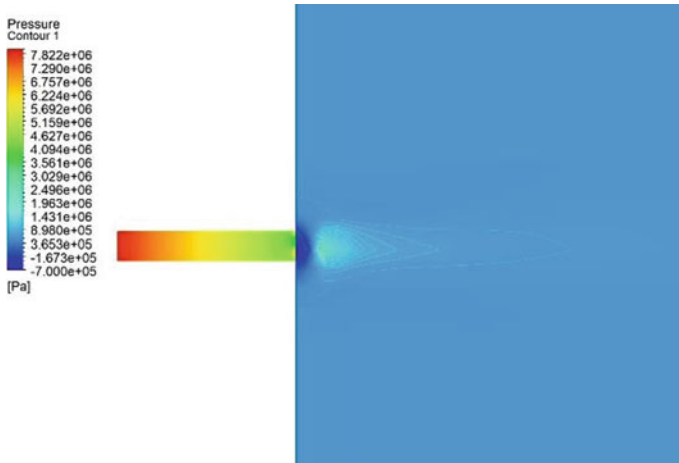


Fig. 10 Pressure contour for aspect ratio 1.6

5 Conclusions

The present study aims to investigate the spray characteristics and fuel droplet atomization performance of the test fuels—diesel and biodiesel, by varying the aspect ratios. The spray characteristics of diesel and ethanol–diesel blend were determined numerically.

The investigation led to the following conclusions:

- i. The variation of aspect ratio in diesel injector is recognized to play an important role in spray characteristics and formation.
- ii. Increasing the aspect ratio enhances turbulence, which causes cavitation in the chamber, hence, increasing the spray angle.
- iii. Due to lower viscosity and density, a lower SMD reduction of up to 28.04% for the ethanol–diesel blend is observed. De Brouckere Diameter also showed a similar trend, declining by 28.63%.
- iv. The spray cone angle was observed to be influenced by the aspect ratio of the elliptical nozzle shape with minimum spray angle in circle being 12.32° and maximum spray angle of 16.30° in case of Elliptical C.
- v. Fuel with higher viscosity, i.e., diesel, does not easily breakup in to smaller droplets. The smaller size of the droplet can improve spray atomization and air–fuel mixing, which is possible in the case of ethanol–diesel blend.

References

1. Som S, Longman DE (2012) Influence of nozzle orifice geometry and fuel properties on flow and cavitation characteristics of a diesel injector. *Fuel Inject Autom Eng* 14:112–126
2. Chen PC, Wang WC (2013) Spray and atomization of diesel fuel and its alternatives from a single-hole injector using a common rail fuel injection system. *Fuel* 103:850–861
3. Iliev S (2018) Comparison of ethanol and methanol blending with gasoline using engine simulation. *Biofuels Challenges Opport*
4. Bannikov M (2015) Effect of alcohol additives on diesel engine performance and emissions. *Mater Methods Technol* 9:8–19
5. Shervani-Tabar MT, Sheykhvazayefi M, Ghorbani M (2013) Numerical study on the effect of the injection pressure on spray penetration length. *Appl Math Model* 37:7778–7788
6. Yu S, Yin B, Deng W, Jia H, Ye Z, Xu B, Xu H (2018) Experimental study on the spray characteristics discharging from elliptical diesel nozzle at typical diesel engine conditions. *Fuel* 221:28–34
7. Yin B, Xu B, Jia H, Yu S (2020) The effect of elliptical diesel nozzles on spray liquid-phase penetration under evaporative conditions. *Energies* 13:2234
8. Wang Z, Li L (2020) Effects of different ethanol/diesel blending ratios on combustion and emission characteristics of a medium-speed diesel engine. *Processes*
9. Singhal AK (2002) Mathematical basis and validation of the full cavitation model. *J Fluids Eng CFD Res Corp J Fluids Eng* 124:617–624
10. Shervani-Tabar MT et al (2012) Numerical study on the effect of the cavitation phenomenon on the characteristics of fuel spray. *Math Comput Modell* 56:105–117
11. Som S, Ramirez AI et al (2010) Effect of nozzle orifice geometry on spray, combustion, and emission characteristics under diesel engine conditions. *Fuel* 90:1267–1276
12. Sun Y, Hooman ZGK (2019) Cavitation in diesel fuel injector nozzles and its influence on atomization and spray. *Chem Eng Technol* 42:6–29

Numerical Simulation of Gasification and Plasma Pyrolysis Process for Lignite Coal: A Comparative Study



Sidhartha Sondh, Darshit S. Upadhyay, Sanjay Patel, and Rajesh N. Patel

Abstract Computational fluid dynamics is a special tool for modeling thermochemical processes for process parameter optimization. The present study is a comparative study of the gasification and plasma pyrolysis process of lignite coal. Three temperatures (1023, 1123, 1223 K) are selected for the gasification process and a similar is done for the plasma pyrolysis (1223, 1323, 1423 K). The obtained results are compared with the experiment literature available. The RMSE approach was used for checking the accuracy of the model. The accuracy was observed to be appreciable. The composition of the syngas is compared for all the cases. It was observed that the concentration of hydrogen and carbon monoxide is found to be rich in plasma pyrolysis with an average of 43.4% as compared to 13.5% for gasification. The plasma pyrolysis process offered better results compared to the gasification process as it offered a higher H_2/CO ratio and $(H_2 + CO)$ factor. The CO/CO_2 ratio also increased for the plasma pyrolysis process with an increase in temperature.

Keywords Computational fluid dynamics · Gasification · Pyrolysis · Plasma pyrolysis · Thermochemical process

1 Introduction

Thermochemical processes such as gasification and pyrolysis are commonly known for energy generation and waste treatment. Due to the huge initial investment and complex process, it is not feasible to carry out experimental research on all the thermochemical processes together. In such an instance, computational fluid dynamics (CFD) emerges as a potential tool for researchers [1]. It also helps in optimizing

S. Sondh · D. S. Upadhyay (✉) · R. N. Patel

Department of Mechanical Engineering, Institute of Technology, Nirma University, Ahmedabad, Gujarat, India

e-mail: Darshitupadhyay@yahoo.com

S. Patel

Department of Chemical Engineering, Institute of Technology, Nirma University, Ahmedabad, Gujarat, India

the designs and other parameters for such processes without involving any major investments [2]. The CFD can also be a useful tool in making the thermochemical processes environment-friendly. Different cases can be simulated to find an effective method for limiting pollutant emissions and improving the overall health of the environment.

Gasification is a widely used thermochemical process for energy production using biomass, coal, municipal solid waste (MSW), etc. [3]. The pyrolysis process also offers the option of energy generation from the above-mentioned feedstocks [4]. The absence of oxygen in the pyrolysis process makes it a more suitable option due to the limited formation of harmful products such as carbon dioxide (CO_2), SO_x , NO_x , PAHs. ANSYS Fluent V17.0 software is used to carry out the simulations of the lignite coal gasification and pyrolysis at different temperatures. The experimental results of lignite gasifications are compared with the CFD simulation results for both processes.

The syngas or producer gas obtained from these thermochemical processes is a mixed gas comprising carbon monoxide (CO), hydrogen (H_2), CO_2 , methane (CH_4), etc. This mixed gas is very valuable and can be used as fuel for cooking and energy generation in the form of electricity and heat [5].

2 Literature Review and Objective

Thermochemical processes are the new way of handling wastes and obtaining useful products. The processes are effective options for meeting the energy demand of the country. Gasification is a globally used technology for generating energy from coal [6]. In the gasification process, the coal is partially oxidized due to the controlled presence of air, oxygen, steam, and CO_2 . Since the presence of oxygen is limited, the process is always under the control and can be solved for different equivalent ratios [7]. The other process considered in this research is pyrolysis. The process of pyrolysis is a new technology that is used for purposes such as waste treatment, energy generation, and oil generation. Pyrolysis is majorly subdivided into three major categories: slow pyrolysis, fast pyrolysis, and flash pyrolysis [8]. However, another category of thermal plasma pyrolysis is also practiced in the industry [9]. The type of feedstock and reactor also influences the thermochemical process. The feedstock can be any waste, biomass, coal, plastics, etc. There are many types of reactors which include downdraft, updraft, fluidized bed, etc. [10]. In this research, fixed bed downdraft reactor is chosen for the analysis.

CFD is an effective tool that is widely used to predict the results of thermochemical processes. Much research focusing on thermochemical processes has been effectively modeled using the CFD tools for optimizing various process parameters. The present research is focused on modeling the two thermochemical processes—gasification and plasma pyrolysis of lignite coal. The processes are modeled for three temperatures 1023, 1123, and 1223 K for gasification whereas that of plasma pyrolysis is 1223, 1323, and 1423 K. The operating temperature range of plasma pyrolysis is higher than

the gasification due to the high working temperature. The mixed gas obtained from both processes is analyzed and compared with the experimental data available. The study highlights the importance of CFD in the optimization of process parameters.

3 Materials and Methods

The fuel for the gasification process was chosen to be lignite coal. The ultimate and proximate analysis for the coal was also conducted and it is mentioned in Table 1. The experiments on lignite coal gasification were carried out at three different temperatures 1023, 1123, and 1223 K.

The composition of the syngas was analyzed using the gas chromatography facility for the syngas sample for each temperature run. These sample data are used to compare and verify the simulation results obtained from the ANSYS Fluent software.

3.1 CFD Modeling

The geometry of the reactor was modeled using the Parametric CREO 3.0 software. The next step in the simulation process is to create the mesh in the reactors. The meshing is done on the model to make a problem more approachable and convenient using the finite element techniques. It breaks the whole domain into small elements and solves the problem at each node. The meshing of the reactor is done in ANSYS ICEM software. For the surface mesh, all triangular elements are used (23,256 elements) Fig. 1, whereas, for the volume generation, hexahedral elements are used (179,821 elements) Fig. 2. The orthogonal quality of all the elements was duly found to be acceptable (> 0.3).

Table 1 Lignite coal: ultimate and proximate analysis data

Ultimate analysis ^a		Proximate analysis ^b	
Carbon	37.80	Volatile matter	42.07
Hydrogen	4.93	Ash	15.11
Nitrogen	1.625	Moisture	11.79
Sulphur	0.141	Fixed carbon ^c	31.03
Oxygen	40.394		

^a Test method IS 1350 (Part II)-1970

^b Test method IS 1350 (Part I)-1984

^c By difference